

www.acsami.org Research Article

# Extracellular Matrix-Derived Biophysical Cues Mediate Interstitial Flow-Induced Sprouting Angiogenesis

Chia-Wen Chang,<sup>†</sup> Hsiu-Chen Shih,<sup>†</sup> Marcos G. Cortes-Medina, Peter E. Beshay, Alex Avendano, Alex J. Seibel, Wei-Hao Liao, Yi-Chung Tung,\* and Jonathan W. Song\*



Cite This: https://doi.org/10.1021/acsami.2c15180



**ACCESS** I

III Metrics & More

Article Recommendations

Supporting Information

ABSTRACT: Sprouting angiogenesis is orchestrated by an intricate balance of biochemical and mechanical cues in the local tissue microenvironment. Interstitial flow has been established as a potent regulator of angiogenesis. Similarly, extracellular matrix (ECM) physical properties, such as stiffness and microarchitecture, have also emerged as important mediators of angiogenesis. However, the interplay between interstitial flow and ECM physical properties in the initiation and control of angiogenesis is poorly understood. Using a three-dimensional (3D) microfluidic tissue analogue of angiogenic sprouting with defined interstitial flow superimposed over ECM with well-characterized physical



properties, we found that the addition of hyaluronan (HA) to collagen-based matrices significantly enhances sprouting induced by interstitial flow compared to responses in collagen-only hydrogels. We confirmed that both the stiffness and matrix pore size of collagen-only hydrogels were increased by the addition of HA. Interestingly, interstitial flow-potentiated sprouting responses in collagen/HA matrices were not affected when functionally blocking the HA receptor CD44. In contrast, enzymatic depletion of HA in collagen/HA matrices with hyaluronidase (HAdase) resulted in decreased stiffness, pore size, and interstitial flow-mediated sprouting to the levels observed in collagen-only matrices. Taken together, these results suggest that HA enhances interstitial flow-mediated angiogenic sprouting through its alterations to collagen ECM stiffness and pore size.

KEYWORDS: microvessel analogue, microfluidics, vascular function, stiffness, pore size, hyaluronidase

#### 1. INTRODUCTION

Angiogenesis, or the extension or expansion of pre-existing blood vessel networks, is essential for several physiological and pathological processes, such as wound healing, inflammation, and cancer. 1-3 During angiogenesis, endothelial cells (ECs) residing in a blood vessel wall undergo morphogenesis to form an angiogenic sprout.<sup>4</sup> Newly formed blood vessels by angiogenesis provide nutrients and oxygen to growing tissues. Pathologies, such as cancer, are characterized by uncontrolled angiogenesis that is initiated and supported by cues arising from the host tissue or microenvironment. Several microenvironmental cues are known to regulate angiogenesis, including biomolecular signaling, biophysical properties of the extracellular matrix (ECM), and biomechanical fluid forces.<sup>7,8</sup> Therefore, because of the broad implications of angiogenesis in health and disease, there is significant interest in understanding the interplay of microenvironmental determinants of EC behavior during neo-vessel outgrowth.

Numerous biomolecules, such as vascular endothelial growth factor (VEGF), <sup>4</sup> C–X–C motif chemokine 12 (CXCL12), <sup>9</sup> and sphingosine-1-phosphate (S1P), <sup>10</sup> have firmly been established as key controllers of vascular morphogenesis. More recently, fluid mechanical forces associated with blood flow have emerged as important regulators of angiogenesis and vascular functions, as either standalone mediators or co-

determinants of biomolecular-induced sprouting.  $^{11,12}$  Of these fluid forces, slowly moving fluid flow across the vessel wall as a result of interstitial plasma flow has been shown to be a potent regulator of angiogenic sprouting.  $^{13,14}$  Interstitial flow is often elevated in tumor and inflammatory microenvironments as a result of heightened pressure gradients within the interstitium.  $^{15}$  Interestingly, multiple studies have confirmed that interstitial flow-mediated angiogenic sprouting preferentially occurs when flow is oriented against the direction of sprouting,  $^{16}$  with this process mediated by delocalization of vascular endothelial (VE)-cadherin cell—cell adhesions,  $^{17}$  small GTPase RhoA,  $^{18}$   $\alpha_{\nu}\beta_{3}$  integrins,  $^{19}$  and other mechanisms.

The composition of the ECM has a profound influence on the biophysical properties of tissue, such as mechanical stiffness, microarchitecture, and transport efficiency of nutrients and drug molecules.<sup>20</sup> Moreover, dysregulated composition and architecture of the ECM are identified as characteristic of tumors,<sup>21,22</sup> fibrosis,<sup>23</sup> and other pathologies.

Received: August 23, 2022 Accepted: February 28, 2023



**ACS Applied Materials & Interfaces** 

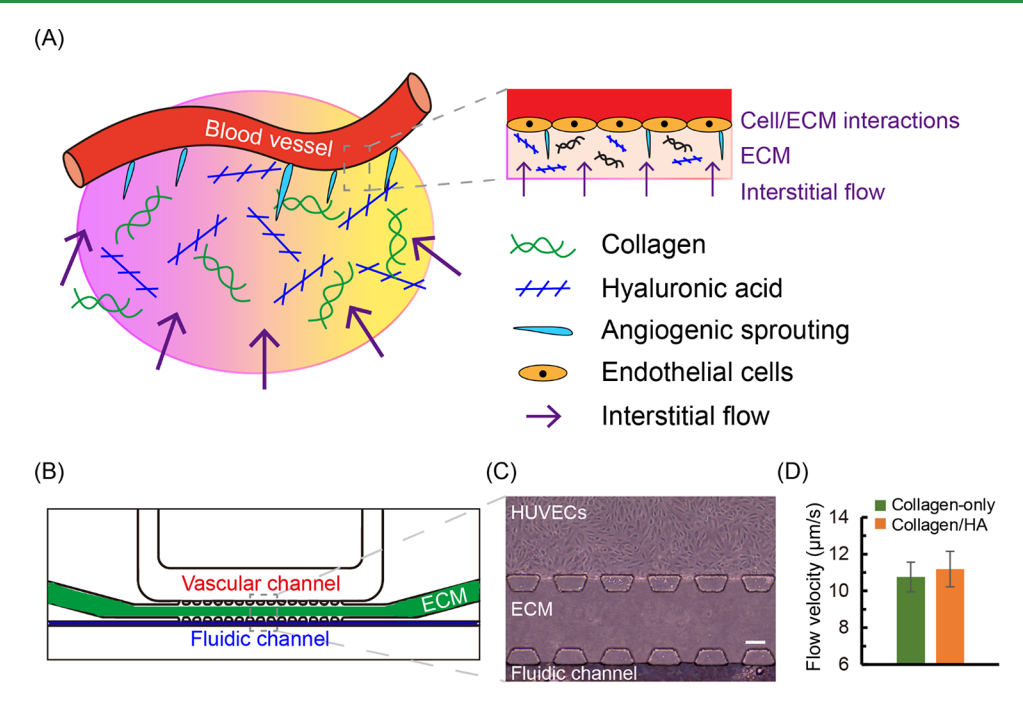


**Figure 1.** 3D biomimetic microfluidic microvessel model for studying interstitial flow-mediated endothelial sprouting. (A) Schematic of interstitial flow-mediated angiogenic sprouting in the tissue microenvironment. (B) Schematic of the developed microfluidic microvessel analogue for studying interstitial flow-induced angiogenic sprouting. (C) Phase-contrast image of HUVECs cultured in the microfluidic microvessel analogue. Scale bars =  $80 \ \mu m$ . (D) Interstitial flow velocity in the microvessel of collagen-only and collagen/HA ECM. The data were expressed as the mean  $\pm$  standard error of the mean (n = 5 for collagen-only gel, and n = 7 for collagen/HA matrices).

For example, increased levels of fibrillar collagen (e.g., types I and III) and non-fibrillar components, such as proteoglycans and glycosaminoglycans (GAGs) (e.g., hyaluronan or HA), in the tumor ECM are characteristic of aggressive or desmoplastic tumors.<sup>24</sup> Recent studies have implicated the composition and physical properties (e.g., stiffness and microarchitecture) of the ECM as important mediators of angiogenesis and microvessel function. For instance, increased tissue stiffness as a result of matrix cross-linking promotes vessel outgrowth and decreased vessel barrier function.<sup>25</sup> Importantly, these responses that were indicative of a tumor vasculature phenotype were independent of VEGF stimulation. Another study determined that the porosity of natural and synthetic hydrogel matrices is a key determinant of angiogenic sprout invasion speed and diameter. 26 Recently, our group reported that angiogenesis and vessel permeability responses induced by CXCL12 isoforms were contingent on the type I collagen and HA compositions of the ECM.

Despite the wealth of evidence that interstitial flow, ECM composition, and ECM physical properties mediate angiogenesis, to our knowledge, no study has simultaneously examined the interplay of these factors in coordinating endothelial sprouting. Here, we used a biomimetic threedimensional (3D) microvessel analogue system that couples systematic evaluation of interstitial flow-potentiated angiogenesis with detailed characterization of ECM physical properties determined by the collagen and HA composition. We observed that the addition of HA to collagen matrices significantly enhanced endothelial sprouting against the direction of interstitial flow. However, under static conditions, the addition of HA to collagen-based matrices had no effect on angiogenic sprouting. Interestingly, interstitial flow-potentiated sprouting responses in collagen/HA matrices were not affected when functionally blocking the HA receptor CD44 with an

anti-CD44 antibody. In contrast, enzymatic depletion of HA with hyaluronidase (HAdase) decreased interstitial flow-mediated sprouting in collagen/HA matrices. We confirmed that the stiffness and pore size of collagen-based matrices were increased by the addition of HA. Moreover, in the presence of a broad-spectrum matrix metalloproteinase (MMP) inhibitor (GM6001), interstitial flow-mediated sprouting was significantly higher in collagen/HA versus collagen-only matrices. These results suggest that HA enhances interstitial flow-mediated angiogenic sprouting through its alterations to ECM stiffness and pore size. Collectively, our study provides novel insights into the role of the biophysical properties of the ECM in controlling angiogenesis in the presence of interstitial flow.

### 2. RESULTS

2.1. HA Enhances Interstitial Flow-Mediated Sprouting Angiogenesis in Collagen-Based Matrices. A biomimetic microfluidic microvessel analogue system was fabricated using poly(dimethylsiloxane) (PDMS) soft lithography to study the combined effects of interstitial flow and ECM composition on sprouting angiogenesis (Figure 1A). The configuration of the microfluidic device was composed of three parallel microchannels (Figure 1B and Figure S1 of the Supporting Information). The two outer channels were denoted as the "vascular channel" and "fluidic channel". The vascular and fluidic channels flank a localized ECM region (see the Materials and Methods for the dimensions of the engineered microvessel analogue). The vascular channel was fully lined with human umbilical vein endothelial cells (HUVECs) to comprise a microvessel analogue (Figure 1C). The fluidic channel provided a fluid pressure source for the generation of interstitial flow of  $\sim 11 \ \mu \text{m/s}$  (Figure 1D) (see the Materials and Methods). Consequently, interstitial flow was oriented from the fluidic channel, through the ECM

region, and into the vascular channel. With this orientation, interstitial flow was applied against endothelial sprouting from the vascular channel. This interstitial flow orientation was used because numerous studies have shown that endothelial cells preferentially sprout against or opposite the direction of interstitial flow. 16 Interstitial flow is estimated to be at a level of  $\sim 1 \mu \text{m/s}$  in normal tissue. <sup>28</sup> This flow velocity is substantially increased in pathological conditions, such as inflammation and cancer. 8,29 The levels of flow that we impose are in line with previous reports in 3D culture models that reflect pathological values of interstitial flow velocity. 19,30 The central channel was filled with either type I collagen ECM (henceforth referred to as "collagen-only") or a mixture of type I collagen gel and HA<sup>31</sup> (henceforth referred to "collagen/HA"). The concentration of 3 mg/mL type I collagen was used for both collagenonly and collagen/HA ECM in this study. For collagen/HA matrices, HA at a concentration of 1 mg/mL was mixed with collagen gel prior to collagen gelation. Thus, the final collagen/ HA ratio used for this study is 3:1 for the 3 mg/mL collagen condition. The ratio of collagen to HA used in this study is relevant to tumor physiology because it is in line with the collagen/HA composition of breast tumors in vivo. 32

To identify the effects of ECM composition on angiogenic sprouting, we first compared sprouting in collagen-only ECM and collagen/HA matrices under static conditions using our HUVEC-lined microfluidic vessel analogue system. HUVECs did not show observable sprouting in both collagen-only ECM and collagen/HA matrices after 3 days of static culture (Figure 2 and Figure S2 of the Supporting Information). Using the

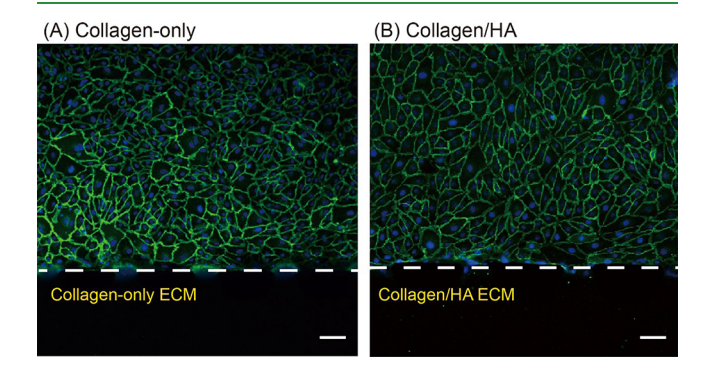
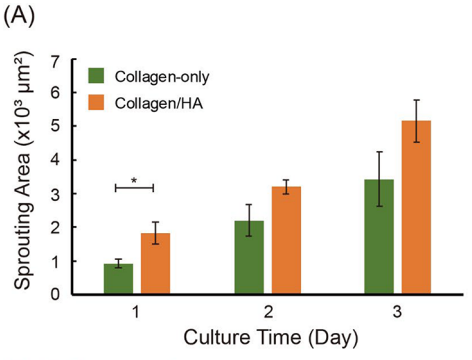
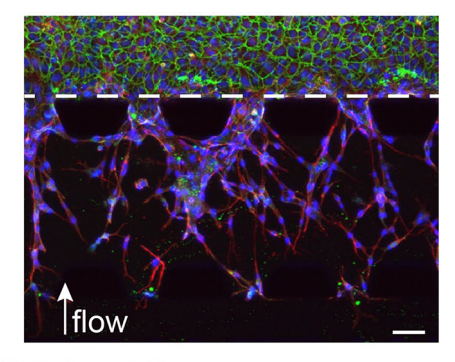


**Figure 2.** Endothelium of HUVECs in the microfluidic microvessel analogue under static conditions on day 3. VE-cadherin junction protein (green) and DAPI (blue) staining of microvessels in (A) collagen-only and (B) collagen/HA matrices under static conditions. Dash white lines indicate the ECM/cell interfaces (scale bars =  $50 \mu m$ ).

same device configuration described in the present study, we observed no difference in cell coverage, cell morphology, and expression of VE-cadherin junctions for the HUVECs grown on collagen-only versus collagen/HA ECM. These results demonstrate that introduction of HA into the collagen-based ECM did not prompt HUVEC sprouting under static conditions. Typically, angiogenesis is coincident with increased vessel permeability, and we previously showed that introduction of HA into collagen-based ECM stabilizes vessel barrier function under static conditions. In contrast, interstitial flow applied against the endothelium of the vessel channel induced HUVEC sprouting for both the collagen-only and collagen/HA matrices (Figure 3). For collagen-only ECM, the average sprouting area increased from 914  $\mu$ m<sup>2</sup> on day 1 to



(B) Collagen-only



(C) Collagen/HA

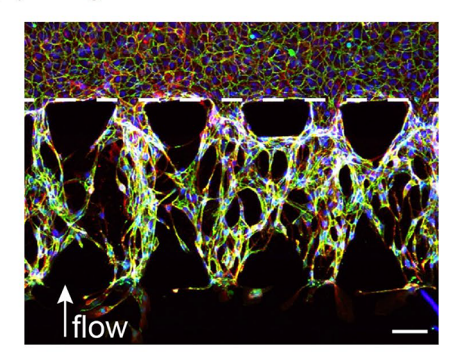


Figure 3. Sprouting angiogenesis mediated by interstitial flow in collagen-only and collagen/HA matrices. (A) Average sprouting area of microvessels in both collagen-only and collagen/HA matrices. The morphology of sprouting in the microvessel analogue is assessed by staining VE-cadherin junction protein (green), F-actin (red), and DAPI (blue) of (B) collagen-only and (C) collagen/HA metrices. The white arrow indicates the direction of interstitial flow. The data were expressed as the mean  $\pm$  standard error of the mean (n=5). One-way ANOVA followed by a post hoc unpaired, two-tailed Student's t test was performed to evaluate the statistical significance.  $\ast$  indicates a p value of <0.05. Dash white lines indicate the ECM/cell interfaces (scale bars = 50  $\mu \rm m$ ).

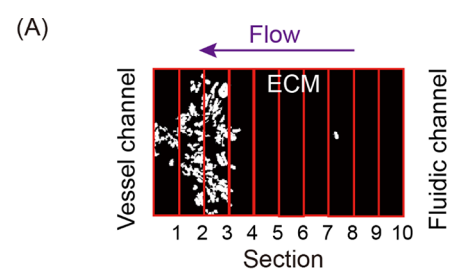
3429  $\mu m^2$  on day 3. For collagen/HA ECM, the average sprouting area increased from 1835  $\mu m^2$  on day 1 to 5158  $\mu m^2$  on day 3 (Figure 3A). These results confirm that interstitial flow promotes angiogenesis when applied against the direction of sprouting. However, it is notable that interstitial flow significantly increased HUVEC sprouting for the collagen/HA matrices by ~2-fold compared to the collagen-only ECM on day 1. These results suggest that the addition of HA to collagen-based ECM promotes sprouting of the microvessels in the presence of interstitial flow (Figure 3A).

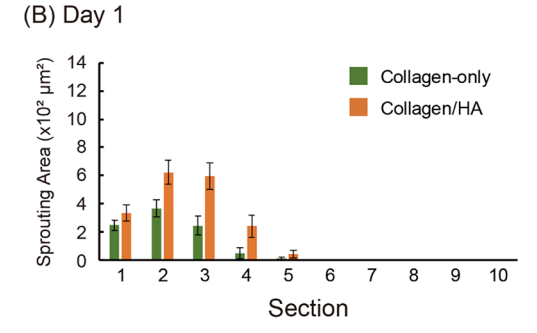
2.2. HA Promotes Interstitial Flow-Induced Sprout Elongation in Collagen-Based Matrices. Interstitial flow

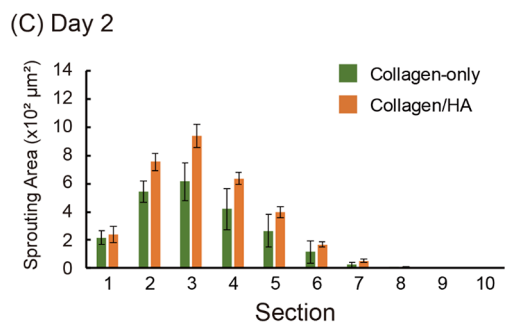
has been shown to be necessary for sustaining endothelial sprout elongation in collagen-only ECM.<sup>12</sup> Interestingly, we observed increased sprout elongation in response to interstitial flow in collagen/HA ECM versus collagen-only ECM. Namely, at day 3, some of the HUVEC sprouts in the collagen/HA ECM reached the distal fluidic channel, while HUVEC sprouts in the collagen-only ECM remained within the ECM compartment (panels B and C of Figure 3). These observations prompted us to compare interstitial flow-mediated sprout elongation in the collagen-only and collagen/HA matrices over multiple days. For this comparison, we set 10 equally divided regions of the ECM. Each section was assigned a number ranging from 1 (proximal endothelium/ECM interface) to 10 (distal fluidic channel) (Figure 4A). On day 1, interstitial flowpromoted sprouting in the collagen/HA ECM was more advanced compared to the collagen-only ECM. For the collagen/HA ECM, most of the sprouting was in sections 2-4, while most of the sprouting for the collagen-only ECM was distributed in sections 1–2 (Figure 4B). Sprout elongation in the collagen/HA ECM continued to be more advanced compared to the collagen-only ECM for days 2 and 3 (panels C and D of Figure 4). These results imply that the addition of HA to collagen-based ECM enhances endothelial sprout elongation in response to interstitial flow over the observed time frame of 3 days.

2.3. Interstitial Flow-Induced Sprouting Is Partially Dependent upon MMP Activity. Furthermore, we assessed the role of matrix metalloproteinases (MMPs) on interstitial flow-induced sprouting into collagen-only and collagen/HA matrices. MMPs are known regulators of sprouting angiogenesis by cleaving peptide bonds of ECM proteins, including collagens. 33,34 In addition, MMPs have been shown to be involved in interstitial flow-mediated HUVEC sprouting in collagen-only ECM. 11,35 We tested the effect of inhibiting MMPs with a full spectrum inhibitor of MMP activity (20  $\mu$ M, GM6001, Millipore Sigma). Inhibition of MMP activity could partially impede interstitial flow-mediated sprouting in both collagen-only and collagen/HA matrices (panels A and B ofFigure 5). However, in the presence of GM6001, the normalized number of sprout percentage in the collagen/HA ECM (105.2%) was significantly higher than that in the collagen-only ECM (82.5%) (see the Materials and Methods for the normalized number of sprout percentage) (Figure 5C). Similarly, in the presence of GM6001, the average sprouting area from the microvessel analogue into the collagen/HA ECM  $(765 \mu m^2)$  was also significantly higher than the average sprouting area into the collagen-only ECM (467  $\mu$ m<sup>2</sup>) on day 1 (Figure 6). In addition, the average sprouting area for the GM6001-treated microvessels was significantly less for both the collagen-only and collagen/HA matrices compared to their respective interstitial flow controls (Figure 6). We confirmed that GM6001 treatments did not promote angiogenic sprouting at static conditions for both collagen-only and collagen/HA matrices (Figure S3 of the Supporting Information). Our results for the GM6001-treated microvessels agree with the observation from a previous report that interstitial flow-induced sprouting is partially dependent upon MMP activity. 11

2.4. Hyaluronidase but Not Anti-CD44 Inhibits Interstitial Flow-Induced Sprouting in Collagen/HA Matrices. The observed enhancement in angiogenic sprouting due to HA and in the context of interstitial flow led us to investigate the involvement of HA-mediated signaling and







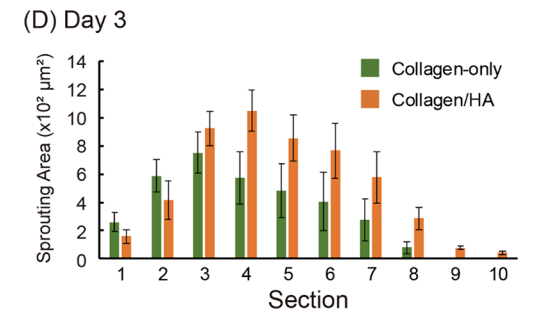


**Figure 4.** Collagen/HA matrices promote the elongation of angiogenic sprouting in interstitial flow-mediated sprouting angiogenesis. (A) Schematic of each section in the ECM compartment. The distribution of angiogenic sprouting in both collagen-only and collagen/HA matrices of the entire ECM compartment on (B) day 1, (C) day 2, and (D) day 3. The data were expressed as the mean  $\pm$  standard error of the mean (n = 5).

biophysical properties. To examine the role HA-mediated signaling, we used a blocking antibody for the HA receptor CD44 (2  $\mu$ g/mL, MA5-13890, Invitrogen). Endothelial CD44 has been shown to be involved with angiogenesis *in vivo*, <sup>36,37</sup> although its role in interstitial flow-promoted sprouting is not known. For collagen-only ECM and in the presence of interstitial flow, anti-CD44 treatment did not significantly affect sprouting activity (943  $\mu$ m<sup>2</sup> versus 914  $\mu$ m<sup>2</sup> for anti-CD44 and untreated control, respectively) (Figure 6). Surprisingly, in collagen/HA ECM, anti-CD44 treatment in the presence of interstitial flow did not affect vessel sprouting

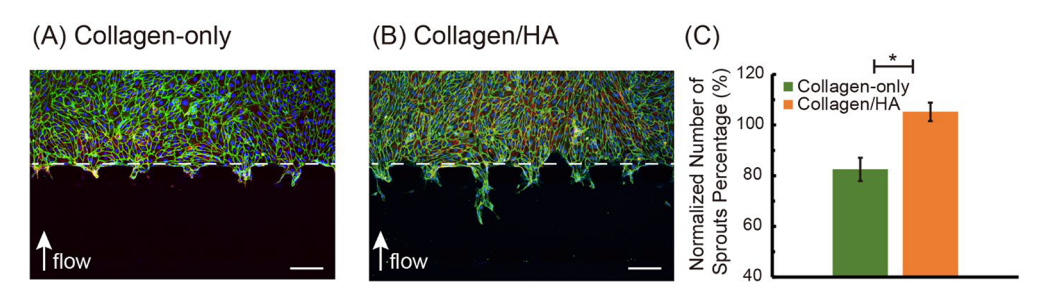
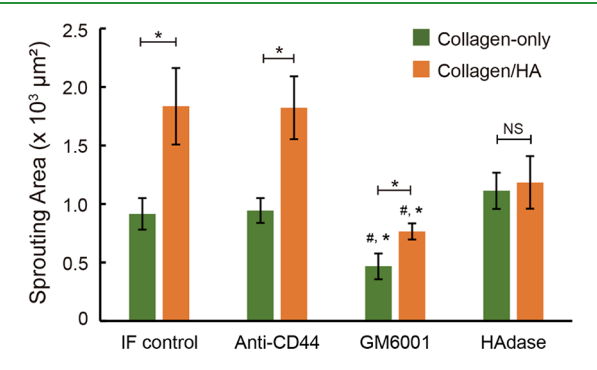


Figure 5. VE-cadherin junction protein (green), actin (red), and DAPI (blue) staining of GM6001-treated angiogenic sprouting of the microvessel analogues in (A) collagen-only and (B) collagen/HA matrices on day 1 culture. (C) Normalized number of sprout precentage of GM6001-treated HUVEC sprouts of microvessels in both collagen-only and collagen/HA matrices. The white arrow indicates the direction of interstitial flow. The data were expressed as the mean  $\pm$  standard error of the mean (n = 3). One-way ANOVA followed by a post hoc unpaired, two-tailed Student's t test was performed to evaluate the statistical significance. \* indicates a p value of <0.05 (scale bars = 150  $\mu$ m).



**Figure 6.** Average sprouting area of HUVECs cultured in microvessel analogues of both collagen-only and collagen/HA matrices in the responses of various pharmaceutical agent treatments (i.e., CD44 blocking, MMP inhibition, and enzymatic matrix degradation) under interstitial flow on day 1. The data were expressed as the mean  $\pm$  standard error ( $n \geq 3$  for all experimental conditions). IF indicates interstitial flow. One-way ANOVA followed by a post hoc unpaired, two-tailed Student's t test was performed to evaluate the statistical significance. # indicates the statistical comparison to the respective IF control. \* indicates a p value of <0.05. NS indicates no significant difference.

(1822  $\mu$ m² versus 1835  $\mu$ m² for anti-CD44 and untreated IF control, respectively). These results suggest that endothelial CD44 signaling was not essentially involved in interstitial flow-potentiated sprouting in collagen/HA matrices. We also tested the effect of co-application of MMP inhibitor (GM6001) and anti-CD44 (Figure S4 of the Supporting Information). In comparison to GM6001-only treated microvessels, co-application of GM6001 with anti-CD44 did not significantly reduce sprouting in the presence of interstitial flow for both the collagen-only and collagen/HA matrices. These results suggest that sprouting inhibition in the presence of interstitial flow as a result of the combinatorial treatment of GM6001 and anti-CD44 was attributed to inhibition of MMP activity and not disrupting the engagement of endothelial CD44 with ECM HA.

Moreover, we examined whether the physical presence of HA enhances interstitial flow-mediated sprouting. To conduct these studies, we enzymatically degraded HA with 1 mg/mL hyaluronidase (HAdase, Sigma). HAdase, namely, its PEGylated human recombinant form (PEGPH20), has been tested in preclinical and clinical settings for treating stromarich, desmoplastic tumors, such as pancreatic ductal adenocarcinoma (PDAC).<sup>38</sup> In addition, our group has previously shown that HAdase alleviates barriers to convective

drug transport through the interstitial matrix by nullifying extracellular HA synthesis by stromal fibroblasts. 39 With regard to endothelial mechanobiology, HAdase has been used to selectively deplete HA of the endothelial glycocalyx, which resulted in blocking increases in vessel permeability induced by intravascular shear stress. 40 However, the role of HAdase in mediating angiogenesis, especially in the context of interstitial flow, is unclear. Upon treatment with HAdase, the average sprouting area significantly decreased (36%) in the collagen/ HA ECM and in the presence of interstitial flow compared to the untreated condition (Figure 6). These results confirm that the addition of HA significantly enhances interstitial flowmediated angiogenesis, which can be nullified by HAdase treatment. Notably, the average sprouting area for HAdasetreated microvessels in the collagen/HA ECM (1183  $\mu$ m<sup>2</sup>) was comparable to both the HAdase-treated collagen-only ECM (1112  $\mu$ m<sup>2</sup>) and untreated collagen-only control (914  $\mu$ m<sup>2</sup>) (Figure 6). We also verified that both CD44 and HAdase did not promote sprouting for both collagen-only and collagen/ HA under static conditions (Figure S3 of the Supporting Information). These results show that inhibition of interstitial flow-mediated sprouting by HAdase is contingent on HA present in the ECM.

2.5. HAdase but Not GM6001 Alters the Mechanical and Structural Properties of Collagen/HA Matrices. Next, we investigated the effects of GM6001 and HAdase treatment on the biophysical properties of acellular ECM hydrogel mixtures (i.e., collagen-only and collagen/HA). These studies were motivated by our results that GM6001 and HAdase but not anti-CD44 treatment significantly inhibit interstitial flow-mediated sprouting of the HUVEC microvessel analogues in collagen/HA ECM (Figure 6). We hypothesized that alterations to biophysical properties as a result of the addition of HA to collagen-based matrices mediate interstitial flow-promoted sprouting. The biophysical properties of the ECM that we characterized were the mechanical stiffness and the microstructural parameter of the mean matrix pore size. We characterized these ECM properties because they have been implicated in regulating endothelial sprouting, although under static culture conditions only. 25,26 To characterize the stiffness profiles of the acellular ECM hydrogel mixtures, we used indentation testing, as previously described by our group.<sup>27,41</sup> To characterize the mean matrix pore size, we employed confocal reflectance microscopy and image analysis techniques described previously by our group.<sup>41</sup>

We first benchmarked changes in mechanical and microstructural properties of untreated collagen-only and collagen/ HA matrices. The measured stiffness for the 3 mg/mL collagen-only gel was 3.15 kPa (Figure 7). The addition of

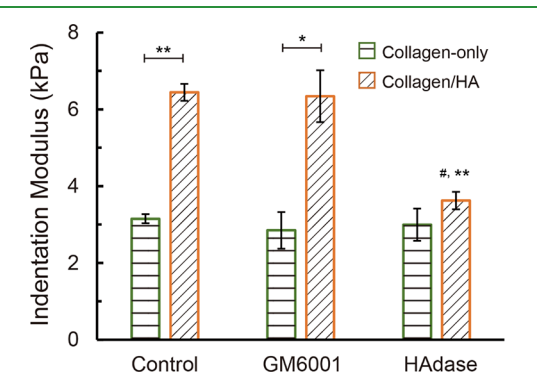


Figure 7. ECM stiffness characterization. Indentation modulus of both collagn-only and collagen/HA matrices in various experimental conditions (MMP inhibition and enzymatic matrix degradation). The biochemical treatment was applied for 24 h before indentation testing was performed. The data were expressed as the mean ± standard error of the mean  $(n \ge 3 \text{ for all experimental conditions})$ . One-way ANOVA followed by a post hoc unpaired, two-tailed Student's t test was performed to evaluate the statistical significance. \* and \*\* indicate p values of <0.05 and <0.01, respectively. # indicates statistical comparison to the collagen/HA control.

HA (1 mg/mL) to the collagen-only gel increased the measured stiffness by approximately 2-fold to 6.44 kPa (Figure 7). These stiffness measurements were in line with our previous reports for the same ECM compositions. 27,41 Moreover, the addition of HA to the collagen-based ECM significantly increased the mean pore size by 13% from 1.70 to 1.92  $\mu$ m compared to collagen-only ECM (Figure 8). We previously reported a similar outcome on the matrix pore size when comparing the same ECM compositions.<sup>41</sup> The increase in the collagen matrix pore size may be attributed to HAinduced swelling, 42 whereas HA associating around the collagen fibers during collagen fibrillogenesis may cause an increase in the fiber radius and ECM stiffness.<sup>43</sup> When integrating the endothelial sprouting results (Figure 6) with the biophysical measurements (Figures 7 and 8), our findings show that the enhancement in interstitial flow-promoted sprouting as a result of the addition of HA to collagen-based ECM correlates with HA-induced increases in the ECM stiffness and matrix pore size.

Subsequently, we confirmed that the addition of GM6001 to acellular collagen-only and collagen/HA did not significantly change the stiffness measurements for collagen-only (2.85 kPa) and collagen/HA (6.34 kPa) compared to the respective untreated control conditions (3.15 and 6.44 kPa) (Figure 7). In addition, GM6001 did not significantly alter the mean matrix pore size for both collagen-only (1.70  $\mu$ m) and collagen/HA (2.06  $\mu$ m) matrices compared to the corresponding untreated conditions for these ECM hydrogel mixtures (1.70  $\mu$ m for collagen-only and 1.92  $\mu$ m for collagen/HA, respectively) (Figure 8). Because GM6001 is an inhibitor of cell-secreted MMPs, we did not expect this pharmacological agent to alter the mechanical and structural properties of acellular matrices. These results imply that partial inhibition of interstitial flow-potentiated endothelial sprouting by GM6001 (Figure 6) was due to blocking the MMP activity and not attributed to direct modifications to the ECM mechanical and structural properties. Furthermore, we also confirmed that

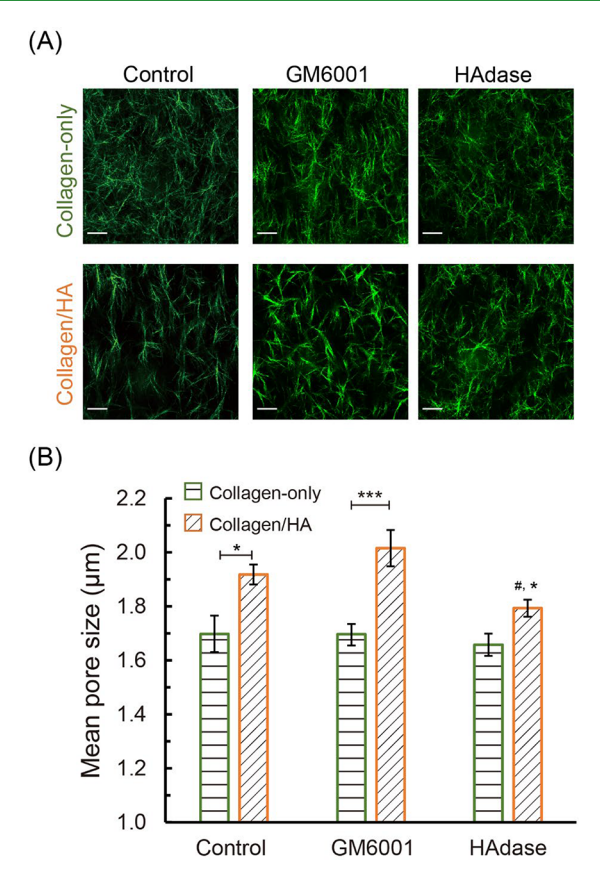


Figure 8. ECM pore size characterization. (A) Reflectance confocal microscopic images of both collagen-only and collagen/HA matrices in various experimental conditions (MMP inhibition and enzymatic matrix degradation). The biochemical treatment was performed for 24 h prior to confocal microscopy imaging. (B) Quantification of the matrix pore size in various experimental conditions at static conditions  $(n \ge 3 \text{ for all experimental conditions})$ . The data were expressed as the mean ± standard error of the mean. One-way ANOVA followed by a post hoc unpaired, two-tailed Student's t test was performed to evaluate the statistical significance. # indicates statistical comparison to the collagen/HA control. \* and \*\*\* indicate p values of <0.05 and <0.001, respectively (scale bars = 20  $\mu$ m).

GM6001 treatment did not affect the stiffness of both collagenonly and collagen/HA hydrogels laden with endothelial cells (Figure S5 of the Supporting Information). Finally, we characterized the mechanical and structural ECM properties as a result of HAdase treatment. For the collagen-only ECM, as expected, we observed no significant changes in the stiffness profile (3.00 kPa) (Figure 7) and mean matrix pore size (1.66 μm) (Figure 8) as a result of HAdase treatment compared to untreated collagen-only ECM. In contrast, treatment of the collagen/HA ECM with HAdase significantly decreased both the stiffness by 43% from 6.44 to 3.62 kPa and the mean matrix pore size by 7% from 1.92 to 1.79  $\mu$ m (Figures 7 and 8). Moreover, the stiffness of HAdase-treated collagen/HA ECM (3.62 kPa) was comparable to HAdase-treated collagen-only ECM (3.00 kPa) and untreated collagen-only ECM (3.15 kPa). Similarly, the mean matrix pore size of HAdase-treated collagen/HA ECM (1.79 µm) was comparable to HAdasetreated collagen-only ECM (1.66 µm) and untreated collagenonly ECM (1.70  $\mu$ m). Therefore, treatment of collagen/HA ECM with HAdase significantly decreased both the stiffness and mean matrix pore size to levels observed for the collagenonly ECM (both untreated and HAdase-treated conditions).

These results suggest that the selective decrease in interstitial flow-promoted sprouting as a result of HAdase treatment in collagen/HA matrices (Figure 6) may be attributed to HAdase decreasing the stiffness and mean matrix pore size of this ECM hydrogel mixture (Figures 7 and 8).

## 3. DISCUSSION

Composition of the 3D ECM profoundly alters biophysical properties of tissue, such as mechanical stiffness, microarchitecture, and transport efficiency of nutrients and drug compounds. While biophysical properties of tissue can be measured *in vivo*, studying the effects of these properties on angiogenesis *in vivo* remains challenging due to limited experimental control over ECM composition. To overcome this fundamental challenge to studying ECM, our design criteria included rigorous control and detailed characterization of the biophysical properties of the reconstituted ECM-derived hydrogels introduced in our *in vitro* microtissue analogue system for studying angiogenesis. This approach enabled us to define how physical properties of the ECM regulate angiogenesis that is potentiated by interstitial flow.

Our study emphasizes angiogenesis responses due to modifications of the collagen ECM by HA addition. We demonstrate that the pro-angiogenic consequences of HA addition to collagen ECM modifications are realized in the presence of interstitial flow only. Interestingly, we observe that functionally blocking HA-CD44 interactions with anti-CD44 did not affect interstitial flow-induced sprouting in collagen/ HA ECM. This result is in contrast with our previously reported observation that, under static conditions, neutralizing HA-CD44 interactions with anti-CD44 completely restored endothelial sprouting levels in collagen/HA matrices compared to the collagen-only counterpart. These results suggest that, while CD44 is key for controlling HA-mediated angiogenic responses under static conditions, it is not essentially involved in angiogenic responses induced by interstitial flow. This outcome is surprising because the CD44 receptor is known to be mechanosensitive. For example, a recent study showed that CD44 strengthens the monoculture brain endothelial cell barrier function in the presence of intravascular fluid shear stress in vitro.44 Moreover, multiple studies have reported that interstitial flow promotes cancer cell invasion via CD44-mediated mechanisms. 45,46 However, our results suggest that, unlike in cancer cells, CD44 is not essentially involved in endothelial cell sprouting prompted by interstitial flow. In addition, we observed that broad spectrum inhibition of MMPs with GM6001 only partially inhibits interstitial flow-induced sprouting, thereby supporting a previous report that interstitial flow-induced sprouting is partially dependent upon MMP activity. 11 These results in the presence of anti-CD44 and GM6001 inhibitor reinforce the potency of standalone interstitial flow in eliciting angiogenesis, particularly when flow is oriented against the direction of endothelial sprouting. 16-19

In the absence of interstitial flow, we observe that ECM HA inhibits endothelial sprouting. This result is consistent with previous reports that, under *in vitro* static conditions, the addition of HA to collagen ECM inhibits capillary tube formation<sup>47</sup> and enhances vascular barrier function.<sup>44</sup> Indeed, we previously reported that the addition of HA to collagenbased matrices suppresses both vessel sprouting and permeability under static *in vitro* conditions and in the absence of CXCL12 treatment.<sup>27</sup> One possible explanation for these

observed decreases in angiogenic activity under static in vitro conditions is that the addition of HA increases the solid fraction of collagen-based ECM hydrogels. Numerous in vitro studies have reported that, under static conditions, increasing the hydrogel concentration of a single fibrillar ECM constituent (e.g., collagen or fibrin) results in decreased vessel outgrowth. 48-50 These outcomes have been attributed to steric hindrances as a result of the increased density of matrix fibers that preclude ECM deformation, degradation, and remodeling that are necessary for vessel morphogenesis. It was also described that increasing fibrin ECM density limits vessel morphogenesis by hindering molecular diffusion from a proangiogenic source (e.g, stromal fibroblasts).<sup>50</sup> However, unlike with standalone collagen or fibrin ECM, where there is an inverse relationship between the ECM concentration and matrix pore size, we previously reported<sup>41</sup> and confirmed in the present study that the addition of non-fibrillar HA increases the fibrillar collagen matrix pore size as a result of swelling of this GAG constituent.<sup>51</sup> Collectively, these previous findings combined with the results from the present study suggest that the role of HA on angiogenesis is highly contingent on the presence or absence of a pro-angiogenic stimulus, whether biochemical or biophysical in nature.

To our knowledge, this report is the first to describe the important role of the ECM physical properties conferred by HA in regulating interstitial flow-mediated angiogenesis. The significant increase in the mean pore size of collagen/HA versus collagen-only matrices may facilitate the initial extension and sustained elongation of HUVECs into the ECM when prompted to sprout by interstitial flow. It is important to recognize that, while the mean pore size within the matrices used in this study is much smaller than the size of an individual cell, collagen fibers have been shown to be sufficiently deformable to create enough void spaces for endothelial sprout elongation. 52,53 Also, flow-induced shear stress in a 3D matrix strongly depends upon local fiber spacing near the cell surface and likely varies widely, even along individual cell membranes.<sup>54</sup> Thus, modifications in the matrix pore size as a result of HA addition may be coupled to large changes in interstitial flow-induced shear stress on endothelial cells during sprouting. Notable challenges for investigating interstitial flowmediated cell response are the complex microarchitecture of the ECM and the difficulty of accurately measuring shear stresses on cells embedded in it. In addition, it is important to consider that our measurements for the matrix microarchitecture were in acellular collagen-based hydrogels that reflect the initial ECM conditions prior to sprouting morphogenesis and matrix remodeling. Therefore, a limitation of our study is that we cannot account for the dynamic changes in the matrix microarchitecture and stiffness that occur during endothelial sprouting and ECM remodeling. Recently, livecell nanobiosensors have been developed and utilized in 3D biomimetic microfluidic systems for real-time detection of cellsecreted molecules and extracellular ligands. 55,56 Moreover, integration of nanoscale force sensors in microtissue analogue systems will enable measurements of interstitial flow-induced shear stress local to endothelial cells in situ.<sup>57</sup> Therefore, the findings from the present study may prompt future work that incorporates such highly capable biosensor approaches in relevant 3D environments, providing tremendous potential to expand the current knowledge of cell-mediated ECM remodeling responses, such as MMP activity, under controlled biomolecular transport and fluid mechanical conditions.

In the present study, we observed more rapid and sustained interstitial flow-induced endothelial sprouting in collagen/HA versus collagen-only matrices. Therefore, our results suggest that the matrix pore size is the primary ECM physical property that mediates interstitial flow-induced endothelial sprouting. A recent study that used collagen-based microfluidic models to study interstitial flow-mediated breast cancer cell invasion also concluded that the matrix pore size and not stiffness was the primary determinant of cancer cell escape into a vascular-like cavity.<sup>58</sup> We note that the physical properties of collagen-based hydrogels can also be modified using non-enzymatic crosslinking methods that afford tunable stiffness and pore size independent of the collagen concentration. 25,59 Thus, it would be interesting in future studies to incorporate tunable collagen hydrogels with other matrix components into microfluidic systems to further investigate and define the combined effects of interstitial flow and ECM physical properties in orchestrating cancer cell-vascular interactions that lead to intravasation events and metastatic dissemination.

A key finding from our study is that HAdase treatment inhibits interstitial flow-promoted angiogenesis by altering the mechanical and microstructural properties of collagen/HA ECM. HAdase has been used in medical applications for decades, <sup>60</sup> primarily as an adjuvant to accelerate the absorption and dispersion of drugs into tissue, including HA-rich primary tumors and metastases. 1 In the context of neovascularization, HAdase is believed to be a pro-angiogenic stimulus by degrading angiostatic native high-molecular-weight HA into pro-angiogenic HA fragments.<sup>63</sup> However, the specific mechanisms driving these size-dependent effects of HA are largely unknown.<sup>64</sup> Our results suggest that HAdase may confer anti-angiogenic outcomes in HA-rich environments and in the presence of interstitial flow. Because tumor growth is angiogenesis-dependent,<sup>65</sup> immense research efforts have been directed toward developing anti-angiogenic therapies that directly neutralize the induction of angiogenesis by proangiogenic molecules, most prominently VEGF.66 However, even when anti-angiogenic drugs have yielded significant clinical trial results leading to regulatory approval, improvements in patient survival have been disappointingly modest on the order of weeks to months,<sup>67</sup> primarily as a result of intrinsic/extrinsic resistance mechanisms.<sup>68</sup> The results from our study demonstrate biophysical induction of angiogenesis that is independent of biomolecular angiogenic stimulation and suggests that angiogenesis can be manipulated indirectly with enzymatic modifications to the ECM. Interestingly, both soluble 16 and matrix-immobilized 69 VEGF have been shown to cooperate with interstitial flow in promoting endothelial sprouting and capillary morphogenesis. Since ECM HA is known to bind and sequester VEGF, 64 it would be interesting in future work to define the interplay of HA, VEGF, and interstitial flow on angiogenesis. Collectively, the findings from our study point to the need for further investigation in the role of ECM physical properties in regulating angiogenesis and anti-angiogenesis mechanisms.

### 4. CONCLUSION

Using 3D microfluidic biomimicry with detailed characterization of hydrogel scaffolds, we investigated how ECM physical properties influence interstitial flow-mediated sprouting angiogenesis. We observed that the addition of HA to collagen-based hydrogels significantly enhances the initial extension and sustained elongation of endothelial sprouting

in response to interstitial flow. The increased interstitial flow-induced angiogenic sprouting is partially dependent upon MMP activity. Interestingly, we show that enhancement in interstitial flow-promoted sprouting in collagen/HA matrices was inhibited significantly with physical remodeling of ECM HA by HAdase but not with blocking HA—CD44 interactions. We also show that HA significantly increases the ECM pore size and stiffness of collagen-based matrices. Taken together, these novel findings comprise an important advancement toward refining our understanding of angiogenesis that is mediated by the biophysical microenvironment. Moreover, these results will help inform future developments in proangiogenic biomaterials and *in vitro* disease models (e.g., organs-on-a-chip) for interrogating mechanisms of vessel outgrowth and remodeling.

#### 5. MATERIALS AND METHODS

5.1. Fabrication of the Microfluidic Device. The microfluidic microvessel analogue was designed with a single-layer microfluidic channel patterned with three sets of channels, as shown in Figure 1B and Figure S1 of the Supporting Information. The vascular channel was exploited for endothelial cell culture to form a microvessel. The hydrogel with a specific composition was introduced in the ECM compartment, and the fluidic channel was utilized to apply interstitial flow across the ECM. Three channels were separated by a series of trapezoid micropillars with a pitch of 200  $\mu$ m. The width of openings (i.e., apertures) between the pillars was designed as 50  $\mu$ m to stably confine the hydrogel within the ECM compartment while allowing the endothelial cells to contact the ECM for sprouting. The widths of the vascular and fluidic channels are 500 and 100  $\mu$ m, respectively. The width of the ECM compartment was 300  $\mu$ m for the observation of the endothelial cell sprouting, and the height of the engineered microvessel analogue was approximately 70  $\mu$ m.

The device was fabricated using PDMS soft lithography. Briefly, the basic and curing agent of the PDMS precursor (Dow Chemical Company) was mixed at 10:1 ratio (w/w) and poured onto a mold wafer with the microfluidic channel pattern. Then, the patterned PDMS layer was irreversibly bonded onto a glass slide by plasma oxidation treatment. The assembled microfluidic device was then placed at 65 °C overnight to promote the bonding between PDMS and glass slide. Type I collagen (Corning, Inc.) isolated from rat tail was introduced into the central ECM compartment and polymerized at 37 °C in a humidified incubator overnight prior to cell seeding. HA (purchased from Sigma) was mixed with collagen gel at a concentration of 1 mg/mL HA to prepare collagen/HA matrices. Collagen-only or collagen/HA pre-polymer mixture at 4 °C was pipetted into the central channel of microdevices and incubated overnight in a humidified incubator at 37 °C. Upon the increase of the temperature to 37 °C, the collagen-based mixture self-assembles into a fibrillar hydrogel scaffold. Confocal microscopy was used to confirm fibrillogenesis of collagen-based hydrogels (detailed description in

5.2. Biophysical Characterization of Extracellular Matrices. The mechanical stiffness of ECM hydrogels was measured using the protocols previously reported by our group.  $^{27,41}$  Briefly, 300  $\mu$ L of 3 mg/mL concentration of collagen-only and collagen/HA was casted on the 10.4 mm diameter custom-made polystyrene housing holder. Biochemical treatments, including inhibition of MMP activities (20  $\mu M$  GM6001) and enzymatic matrix degradation of HA (1 mg/mL hyaluronidase), were performed by incubating the ECM hydrogels with 200  $\mu$ L of individual reagents for 1 day in a humidified incubator. Samples were kept immersed in phosphate-buffered saline (PBS) during mechanical testing to maintain the collagen-based gels in a hydrated environment. The stiffness measurement was conducted by the high-precision indentation system (ElectroForce 5500, TA Instruments), which was programmed to indent the gel to up to 40% strain at 10% increasing intervals lasting 300 s each. The peak load responses were automatically recorded and used to calculate

stress using the displacement at each interval and known indenter geometry (diameter of 4.8 mm). Stress responses were automatically recorded corresponding to each strain. The indentation modulus is defined as the ratio of stress over strain. To evaluate the stiffness of GM6001-treated cell-laden hydrogels, HUVECs at the concentration of  $1\times10^6$  cells/mL were well-mixed with pre-polymer solution and incubated 1 day prior to the stiffness measurement.

5.3. Collagen Fiber Imaging and Mean Pore Size Analysis. The collagen fiber of both collagen-only gel and collagen/HA in the microvessel analogues was imaged using confocal microscopy on a Nikon A1R Live Cell Imaging Confocal Microscope via a 40X 1.3 numerical aperture (NA) oil immersion lens controlled with NIS-Elements software. Confocal reflectance stacks of approximately 50  $\mu$ m in height with a z step of 0.59  $\mu$ m were acquired for image analysis (80–90 total images per stack). When imaging, 3 stacks per devices were obtained. The average pore size of the matrix was estimated by use of the MO method. In this approach, the average pore size was quantified by morphological operations on binary images using a house-made MATLAB script. Matrix pore size histograms of individual hydrogels at each condition were also generated to validate the average pore size estimations (Figure S6 of the Supporting Information)

**5.4.** Characterization of Interstitial Flow. To generate interstitial flow, pipette tips with 80  $\mu$ L of culture media were inserted to the two inlets of the fluidic channel. Texas-red conjugated Dextran fluorescent dye was introduced in the same manner as the interstitial flow setup in the cell culture experiments. A time-lapse fluorescent microscope was employed to track the flow of dye into the collagen gel over time. Then, we applied the control volume approach of fluid flux transport to evaluate the average flow velocity. The simplified advection transport equation is

$$\frac{\partial \varphi}{\partial t} = -\nu \frac{\partial \varphi}{\partial x} \tag{1}$$

where  $\psi$ , v, t, and x are the fluorescent intensity of the dye, average flow velocity, time, and distance along the flow direction, respectively. The assumptions here are that (i) flow in the microfluidic device is one-dimensional (i.e., flow across the ECM compartment is only present in the direction perpendicular to channels) and (ii) convective transport is dominant in interstitial flow conditions. Using this method, interstitial flow velocity in the microdevice with the vascular channel lined with HUVECs was  $\sim 10.76$  and  $11.18~\mu m/s$  for the microvessel of collagen-only and collagen/HA matrices, correspondingly.

5.5. Preparation of HUVECs. HUVECs were purchased from Lonza and cultured in endothelial growth medium 2 (EGM-2, Lonza). HUVECs were cultured in T-75 flasks in a humidified cell culture incubator at 37  $^{\circ}C$  and 5%  $CO_{2}$ , with the culture medium being changed every 2 days. Cell passage numbers of 5-12 were used in this study. To improve the biocompatibility of the microfluidic device, the vascular channels were coated with fibronectin solution at a concentration of 100  $\mu$ g/mL at least 30 min prior to cell seeding. HUVECs were harvested from a flask using 0.05% ethylenediaminetetraacetic acid (EDTA)-trypsin (Invitrogen) for 4 min, and the cell suspension was centrifuged at 950 rpm for 4 min. To acquire a monolayer of HUVECs lining the vascular channels, the cell suspension was adjusted to  $\sim 2 \times 10^7$  cells/mL and introduced to the channel by pipetting. The medium was changed every day in the device to ensure better cell attachment and healthy cell growth. For all experiments, treated conditions were introduced after cells had been cultured in the microfluidic device for 1 day to ensure that treatment had no effect on initial cell attachment. For CD44 blocking experiments, trypsinized HUVECs were treated with medium containing CD44 antibody (2 µg/mL, MA5-13890, Invitrogen) for 30 min at room temperature prior to seeding. GM6001 (CC10, Millipore Sigma) was diluted to 20  $\mu$ M in culture medium and introduced to HUVECs cultured in the microvessel analogue for the MMP inhibition experiments. For HAdase treatment, HAdase was diluted to 1 mg/mL in the culture medium and applied to both the fluidic channel and HUVECs cultured in the microvessel analogue. To

generate the interstitial flow, pipette tips with 80  $\mu$ L of medium were inserted to the two inlets of the fluidic channel. The inserted pipette tips were replenished every day to ensure that the pressure head was maintained.

5.6. Sprouting Angiogenesis Assay and Sprouting Elongation Analysis. HUVECs were cultured in microfluidic devices for 3 days using endothelial cell culture medium. Phase-contrast images of sprouts from ECM/vessel interfaces were taken every 24 h, and a house-made MATLAB code was used to evaluate the specific sprouting area of each device. To evaluate the elongation of angiogenic sprouting, ECM compartment was divided into 10 equal regions and a house-made MATLAB code was applied to analyze the total sprouting area in each ECM region to generate a distribution of the angiogenic sprouting area across the entire ECM compartment. To analyze the sprouting number in MMP inhibition, individual sprouts that originate from the HUVEC/ECM interface and directed toward the opposite side were counted. Cells that were in the middle of the ECM gel but not connected to the HUVEC/ECM interface were excluded. The normalized sprouting number percentage is defined as a percentage of the total sprouting number per device divided by the total number of HUVECs/ECM interface (i.e., aperture) in a device.

5.7. Immunofluorescence Staining. HUVECs cultured in the microvessel analogues were fixed by 4% paraformaldehyde (158127, Sigma-Aldrich) for 15 min at room temperature. Then, the microvessels were permeabilized by incubating with 0.1% Triton X-100 (T9284, Sigma-Aldrich) for 10 min. Subsequently, the microvessels were incubated with 0.1% bovine serum albumin (A7906, Sigma) overnight at 4 °C to avoid non-specific binding. VE-cadherin was stained by incubation with VE-cadherin primary antibody (SC-9989, Santa Cruz Biotechnology) at a 1:125 dilution in Dulbecco's phosphate-buffered saline (DPBS) overnight and washed with 1% Tween 20 (1610781, Bio-Rad Laboratories) subsequently. HUVECs were then stained with Alexa Fluor 488 donkey secondary antibody (A21202, Invitrogen) at a 1:500 dilution in DPBS for 3 h at room temperature. F-actin is labeled with Alexa Fluor 546 Phalloidin (A22283, Invitrogen) at 1:100 in DPBS for 3 h at room temperature. Cell nuclei of HUVECs were stained by 4',6-diamidino-2-phenylindole (DAPI, D1306, Invitrogen) at 1:500 dilution for 15 min. Confocal microscopy was performed on the stained microvessel using a broadband confocal microscope (TCS SP5, Leica Microsystems, Wetzlar, Germany).

**5.8. Statistical Analysis.** Numerical data reported in this manuscript were expressed as the mean  $\pm$  standard error of the mean (SEM). Each experimental condition was performed at least in three replicates to conduct statistical analysis. Variations of all data were statistically analyzed by performing one-way analysis of Variance (ANOVA) followed by a post hoc unpaired, two-tailed Student's t test, executed by OriginLab software. To compare the statistical difference of each experimental condition, the asterisk mark (\*) was applied as \* for a p value of <0.001, and \*\*\* for a p value of <0.001.

## ASSOCIATED CONTENT

## Supporting Information

The Supporting Information is available free of charge at https://pubs.acs.org/doi/10.1021/acsami.2c15180.

Additional experimental details, angiogenic sprouting results, effect of MMP activity on hydrogel stiffness, and pore size distribution of ECM hydrogels (PDF)

## AUTHOR INFORMATION

#### **Corresponding Authors**

ı

Jonathan W. Song — Department of Mechanical and Aerospace Engineering and The Comprehensive Cancer Center, The Ohio State University, Columbus, Ohio 43210, United States; o orcid.org/0000-0002-6991-5298; Email: song.1069@osu.edu

Yi-Chung Tung — Research Center for Applied Science, Academia Sinica, Taipei 115-29, Taiwan; ⊙ orcid.org/ 0000-0002-6170-2992; Email: tungy@gate.sinica.edu.tw

#### **Authors**

Chia-Wen Chang — Department of Chemical and Biomolecular Engineering, The Ohio State University, Columbus, Ohio 43210, United States; orcid.org/0000-0002-0810-8556

Hsiu-Chen Shih – Research Center for Applied Science, Academia Sinica, Taipei 115-29, Taiwan

Marcos G. Cortes-Medina — Department of Biomedical Engineering, The Ohio State University, Columbus, Ohio 43210, United States

Peter E. Beshay — Department of Mechanical and Aerospace Engineering, The Ohio State University, Columbus, Ohio 43210, United States

Alex Avendano – Department of Biomedical Engineering, The Ohio State University, Columbus, Ohio 43210, United States

Alex J. Seibel – Department of Chemical and Biomolecular Engineering, The Ohio State University, Columbus, Ohio 43210, United States

Wei-Hao Liao – Research Center for Applied Science, Academia Sinica, Taipei 115-29, Taiwan

Complete contact information is available at: https://pubs.acs.org/10.1021/acsami.2c15180

#### **Author Contributions**

<sup>†</sup>Chia-Wen Chang and Hsiu-Chen Shih contributed equally to this work.

#### **Notes**

The authors declare no competing financial interest.

#### ACKNOWLEDGMENTS

This work was supported by funding awarded to Jonathan W. Song from a National Science Foundation (NSF) CAREER Award (CBET-1752106), the American Heart Association (15SDG25480000), Pelotonia Junior Investigator Award, the National Heart, Lung, and Blood Institute (NHLBI) (R01HL141941), and The Ohio State University (OSU) Materials Research Seed Grant Program, funded by the Center for Emergent Materials, a NSF-Materials Research Science and Engineering Center (MRSEC) (Grant DMR-1420451), the Center for Exploration of Novel Complex Materials, and the Institute for Materials Research. This work was also supported by funding awarded to Yi-Chung Tung from the Taiwan Ministry of Science and Technology (MOST 109-2221-E-001-002-MY2 and 110-2221-E-001-005-MY3). Partial personnel support through the Mark Foundation for Cancer Research (18-024-ASP) is also acknowledged. Chia-Wen Chang, Peter E. Beshay, and Alex Avendano gratefully acknowledge funding from the Pelotonia Graduate Fellowship Program. Hsiu-Chen Shih was supported by the Technology Elite Cultivation Project from Academia Sinica for the research visit to OSU. Marcos G. Cortes-Medina thanks the support from an OSU Graduate Enrichment Fellowship, a Discovery Scholars Fellowship, and a NHLBI Diversity Supplement. This work was also supported, in part, by the Mary Wieczynski Furnivall Cancer Research Fund. Reflectance confocal microscopic images of collagen-based matrices presented in this

report were generated using instruments and services at the Campus Microscopy and Imaging Facility (CMIF), The Ohio State University. This facility is supported in part by Grant P30 CA016058, National Cancer Institute.

## **■** REFERENCES

- (1) Fiedler, U.; Reiss, Y.; Scharpfenecker, M.; Grunow, V.; Koidl, S.; Thurston, G.; Gale, N. W.; Witzenrath, M.; Rosseau, S.; Suttorp, N.; Sobke, A.; Herrmann, M.; Preissner, K. T.; Vajkoczy, P.; Augustin, H. G. Angiopoietin-2 sensitizes endothelial cells to TNF-alpha and has a crucial role in the induction of inflammation. *Nat. Med.* **2006**, *12* (2), 235–239
- (2) Weis, S. M.; Cheresh, D. A. Tumor angiogenesis: Molecular pathways and therapeutic targets. *Nat. Med.* **2011**, *17* (11), 1359–1370.
- (3) Tonnesen, M. G.; Feng, X.; Clark, R. A. Angiogenesis in wound healing. *J. Invest. Dermatol. Symp. Proc.* **2000**, 5 (1), 40–46.
- (4) Gerhardt, H.; Golding, M.; Fruttiger, M.; Ruhrberg, C.; Lundkvist, A.; Abramsson, A.; Jeltsch, M.; Mitchell, C.; Alitalo, K.; Shima, D.; Betsholtz, C. VEGF guides angiogenic sprouting utilizing endothelial tip cell filopodia. *J. Cell Biol.* **2003**, *161* (6), 1163–1177.
- (5) Pries, A. R.; Secomb, T. W. Making microvascular networks work: Angiogenesis, remodeling, and pruning. *Physiology* **2014**, 29 (6), 446–455.
- (6) Carmeliet, P.; Jain, R. K. Molecular mechanisms and clinical applications of angiogenesis. *Nature* **2011**, 473 (7347), 298–307.
- (7) Gray, K. M.; Stroka, K. M. Vascular endothelial cell mechanosensing: New insights gained from biomimetic microfluidic models. *Semin. Cell Dev. Biol.* **2017**, *71*, 106–117.
- (8) Chang, C. W.; Seibel, A. J.; Song, J. W. Application of microscale culture technologies for studying lymphatic vessel biology. *Microcirculation* **2019**, *26* (8), e12547.
- (9) Zhang, M.; Qiu, L.; Zhang, Y.; Xu, D.; Zheng, J. C.; Jiang, L. CXCL12 enhances angiogenesis through CXCR7 activation in human umbilical vein endothelial cells. *Sci. Rep* **2017**, *7* (1), 8289.
- (10) Cartier, A.; Leigh, T.; Liu, C. H.; Hla, T. Endothelial sphingosine 1-phosphate receptors promote vascular normalization and antitumor therapy. *Proc. Natl. Acad. Sci. U. S. A.* **2020**, *117* (6), 3157–3166.
- (11) Abe, Y.; Watanabe, M.; Chung, S.; Kamm, R. D.; Tanishita, K.; Sudo, R. Balance of interstitial flow magnitude and vascular endothelial growth factor concentration modulates three-dimensional microvascular network formation. *APL Bioeng.* **2019**, *3* (3), 036102.
- (12) Galie, P. A.; Nguyen, D. H.; Choi, C. K.; Cohen, D. M.; Janmey, P. A.; Chen, C. S. Fluid shear stress threshold regulates angiogenic sprouting. *Proc. Natl. Acad. Sci. U. S. A.* **2014**, *111* (22), 7968–7973.
- (13) Kim, S.; Chung, M.; Ahn, J.; Lee, S.; Jeon, N. L. Interstitial flow regulates the angiogenic response and phenotype of endothelial cells in a 3D culture model. *Lab Chip* **2016**, *16* (21), 4189–4199.
- (14) Moya, M. L.; Hsu, Y. H.; Lee, A. P.; Hughes, C. C.; George, S. C. In vitro perfused human capillary networks. *Tissue Eng., Part C* **2013**, *19* (9), 730–737.
- (15) Swartz, M. A.; Lund, A. W. Lymphatic and interstitial flow in the tumour microenvironment: Linking mechanobiology with immunity. *Nat. Rev. Cancer* **2012**, *12* (3), 210–219.
- (16) Song, J. W.; Munn, L. L. Fluid forces control endothelial sprouting. *Proc. Natl. Acad. Sci. U. S. A.* **2011**, 108 (37), 15342–15347.
- (17) Vickerman, V.; Kamm, R. D. Mechanism of a flow-gated angiogenesis switch: Early signaling events at cell-matrix and cell-cell junctions. *Integr. Biol.* **2012**, *4* (8), 863–874.
- (18) Song, J. W.; Daubriac, J.; Tse, J. M.; Bazou, D.; Munn, L. L. RhoA mediates flow-induced endothelial sprouting in a 3D tissue analogue of angiogenesis. *Lab Chip* **2012**, *12* (23), 5000–5006.
- (19) Shirure, V. S.; Lezia, A.; Tao, A.; Alonzo, L. F.; George, S. C. Low levels of physiological interstitial flow eliminate morphogen gradients and guide angiogenesis. *Angiogenesis* **2017**, *20* (4), 493–504.

- (20) Philp, C. J.; Siebeke, I.; Clements, D.; Miller, S.; Habgood, A.; John, A. E.; Navaratnam, V.; Hubbard, R. B.; Jenkins, G.; Johnson, S. R. Extracellular Matrix Cross-Linking Enhances Fibroblast Growth and Protects against Matrix Proteolysis in Lung Fibrosis. *Am. J. Respir. Cell Mol. Biol.* **2018**, *58* (5), 594–603.
- (21) Fenner, J.; Stacer, A. C.; Winterroth, F.; Johnson, T. D.; Luker, K. E.; Luker, G. D. Macroscopic stiffness of breast tumors predicts metastasis. *Sci. Rep.* **2014**, *4*, 5512.
- (22) Conklin, M. W.; Eickhoff, J. C.; Riching, K. M.; Pehlke, C. A.; Eliceiri, K. W.; Provenzano, P. P.; Friedl, A.; Keely, P. J. Aligned collagen is a prognostic signature for survival in human breast carcinoma. *Am. J. Pathol.* **2011**, *178* (3), 1221–1232.
- (23) Marinkovic, A.; Liu, F.; Tschumperlin, D. J. Matrices of physiologic stiffness potently inactivate idiopathic pulmonary fibrosis fibroblasts. *Am. J. Respir. Cell Mol. Biol.* **2013**, 48 (4), 422–430.
- (24) Liu, M.; Tolg, C.; Turley, E. Dissecting the Dual Nature of Hyaluronan in the Tumor Microenvironment. *Front. Immunol.* **2019**, 10, 947.
- (25) Bordeleau, F.; Mason, B. N.; Lollis, E. M.; Mazzola, M.; Zanotelli, M. R.; Somasegar, S.; Califano, J. P.; Montague, C.; LaValley, D. J.; Huynh, J.; Mencia-Trinchant, N.; Negron Abril, Y. L.; Hassane, D. C.; Bonassar, L. J.; Butcher, J. T.; Weiss, R. S.; Reinhart-King, C. A. Matrix stiffening promotes a tumor vasculature phenotype. *Proc. Natl. Acad. Sci. U. S. A.* **2017**, *114* (3), 492–497.
- (26) Wang, W. Y.; Kent, R. N., 3rd; Huang, S. A.; Jarman, E. H.; Shikanov, E. H.; Davidson, C. D.; Hiraki, H. L.; Lin, D.; Wall, M. A.; Matera, D. L.; Shin, J. W.; Polacheck, W. J.; Shikanov, A.; Baker, B. M. Direct comparison of angiogenesis in natural and synthetic biomaterials reveals that matrix porosity regulates endothelial cell invasion speed and sprout diameter. *Acta Biomater.* **2021**, *135*, 260–273.
- (27) Chang, C.-W.; Seibel, A. J.; Avendano, A.; Cortes-Medina, M. G.; Song, J. W. Distinguishing Specific CXCL12 Isoforms on Their Angiogenesis and Vascular Permeability Promoting Properties. *Adv. Healthcare Mater.* **2020**, *9* (4), 1901399.
- (28) Chary, S. R.; Jain, R. K. Direct measurement of interstitial convection and diffusion of albumin in normal and neoplastic tissues by fluorescence photobleaching. *Proc. Natl. Acad. Sci. U. S. A.* **1989**, *86* (14), 5385–5389.
- (29) Wiig, H.; Swartz, M. A. Interstitial fluid and lymph formation and transport: Physiological regulation and roles in inflammation and cancer. *Physiol. Rev.* **2012**, *92* (3), 1005–1060.
- (30) Ng, C. P.; Hinz, B.; Swartz, M. A. Interstitial fluid flow induces myofibroblast differentiation and collagen alignment in vitro. *J. Cell Sci.* **2005**, *118* (20), 4731–4739.
- (31) Kreger, S. T.; Voytik-Harbin, S. L. Hyaluronan concentration within a 3D collagen matrix modulates matrix viscoelasticity, but not fibroblast response. *Matrix Biol.* **2009**, *28* (6), 336–346.
- (32) Netti, P. A.; Berk, D. A.; Swartz, M. A.; Grodzinsky, A. J.; Jain, R. K. Role of extracellular matrix assembly in interstitial transport in solid tumors. *Cancer Res.* **2000**, *60* (9), 2497–2503.
- (33) Quintero-Fabián, S.; Arreola, R.; Becerril-Villanueva, E.; Torres-Romero, J. C.; Arana-Argáez, V.; Lara-Riegos, J.; Ramírez-Camacho, M. A.; Alvarez-Sánchez, M. E. Role of Matrix Metalloproteinases in Angiogenesis and Cancer. Front. Oncol. 2019, 9, 1370.
- (34) Sang, Q. X. Complex role of matrix metalloproteinases in angiogenesis. *Cell Res.* **1998**, 8 (3), 171–177.
- (35) Bazou, D.; Ng, M. R.; Song, J. W.; Chin, S. M.; Maimon, N.; Munn, L. L. Flow-induced HDAC1 phosphorylation and nuclear export in angiogenic sprouting. *Sci. Rep.* **2016**, *6* (1), 34046.
- (36) Cao, G.; Savani, R. C.; Fehrenbach, M.; Lyons, C.; Zhang, L.; Coukos, G.; Delisser, H. M. Involvement of endothelial CD44 during in vivo angiogenesis. *Am. J. Pathol.* **2006**, *169* (1), 325–336.
- (37) Chen, L.; Fu, C.; Zhang, Q.; He, C.; Zhang, F.; Wei, Q. The role of CD44 in pathological angiogenesis. *FASEB J.* **2020**, 34 (10), 13125–13139.
- (38) Provenzano, P. P.; Cuevas, C.; Chang, A. E.; Goel, V. K.; Von Hoff, D. D.; Hingorani, S. R. Enzymatic targeting of the stroma

- ablates physical barriers to treatment of pancreatic ductal adenocarcinoma. Cancer Cell 2012, 21 (3), 418-429.
- (39) Hammer, A. M.; Sizemore, G. M.; Shukla, V. C.; Avendano, A.; Sizemore, S. T.; Chang, J. J.; Kladney, R. D.; Cuitino, M. C.; Thies, K. A.; Verfurth, Q.; Chakravarti, A.; Yee, L. D.; Leone, G.; Song, J. W.; Ghadiali, S. N.; Ostrowski, M. C. Stromal PDGFR-alpha Activation Enhances Matrix Stiffness, Impedes Mammary Ductal Development, and Accelerates Tumor Growth. *Neoplasia* 2017, 19 (6), 496–508.
- (40) Lopez-Quintero, S. V.; Amaya, R.; Pahakis, M.; Tarbell, J. M. The endothelial glycocalyx mediates shear-induced changes in hydraulic conductivity. *Am. J. Physiol.: Heart Circ. Physiol.* **2009**, 296 (5), H1451–H1456.
- (41) Avendano, A.; Chang, J. J.; Cortes-Medina, M. G.; Seibel, A. J.; Admasu, B. R.; Boutelle, C. M.; Bushman, A. R.; Garg, A. A.; DeShetler, C. M.; Cole, S. L.; Song, J. W. Integrated Biophysical Characterization of Fibrillar Collagen-Based Hydrogels. *ACS Biomater. Sci. Eng.* **2020**, *6* (3), 1408–1417.
- (42) Lai, V. K.; Nedrelow, D. S.; Lake, S. P.; Kim, B.; Weiss, E. M.; Tranquillo, R. T.; Barocas, V. H. Swelling of Collagen-Hyaluronic Acid Co-Gels: An In Vitro Residual Stress Model. *Ann. Biomed. Eng.* **2016**, *44* (10), 2984–2993.
- (43) Xin, X.; Borzacchiello, A.; Netti, P. A.; Ambrosio, L.; Nicolais, L. Hyaluronic-acid-based semi-interpenetrating materials. *J. Biomater. Sci., Polym. Ed.* **2004**, *15* (9), 1223–1236.
- (44) DeOre, B. J.; Partyka, P. P.; Fan, F.; Galie, P. A. CD44 mediates shear stress mechanotransduction in an in vitro blood-brain barrier model through small GTPases RhoA and Rac1. *FASEB J.* **2022**, *36* (5), e22278.
- (45) Kingsmore, K. M.; Logsdon, D. K.; Floyd, D. H.; Peirce, S. M.; Purow, B. W.; Munson, J. M. Interstitial flow differentially increases patient-derived glioblastoma stem cell invasion via CXCR4, CXCL12, and CD44-mediated mechanisms. *Integr. Biol.* **2016**, *8* (12), 1246–1260.
- (46) Qazi, H.; Palomino, R.; Shi, Z. D.; Munn, L. L.; Tarbell, J. M. Cancer cell glycocalyx mediates mechanotransduction and flow-regulated invasion. *Integr. Biol.* **2013**, *5* (11), 1334–1343.
- (47) Rooney, P.; Kumar, S.; Ponting, J.; Wang, M. The role of hyaluronan in tumour neovascularization (review). *Int. J. Cancer* **1995**, 60 (5), 632–636.
- (48) Cross, V. L.; Zheng, Y.; Won Choi, N.; Verbridge, S. S.; Sutermaster, B. A.; Bonassar, L. J.; Fischbach, C.; Stroock, A. D. Dense type I collagen matrices that support cellular remodeling and microfabrication for studies of tumor angiogenesis and vasculogenesis in vitro. *Biomaterials* **2010**, *31* (33), 8596–8607.
- (49) Edgar, L. T.; Underwood, C. J.; Guilkey, J. E.; Hoying, J. B.; Weiss, J. A. Extracellular matrix density regulates the rate of neovessel growth and branching in sprouting angiogenesis. *PLoS One* **2014**, *9* (1), e85178.
- (50) Ghajar, C. M.; Chen, X.; Harris, J. W.; Suresh, V.; Hughes, C. C.; Jeon, N. L.; Putnam, A. J.; George, S. C. The effect of matrix density on the regulation of 3D capillary morphogenesis. *Biophys. J.* **2008**, *94* (5), 1930–1941.
- (51) Chen, X.; Chen, D.; Ban, E.; Toussaint, K. C.; Janmey, P. A.; Wells, R. G.; Shenoy, V. B. Glycosaminoglycans modulate long-range mechanical communication between cells in collagen networks. *Proc. Natl. Acad. Sci. U. S. A.* **2022**, *119* (15), e2116718119.
- (52) Vaeyens, M. M.; Jorge-Penas, A.; Barrasa-Fano, J.; Steuwe, C.; Heck, T.; Carmeliet, P.; Roeffaers, M.; Van Oosterwyck, H. Matrix deformations around angiogenic sprouts correlate to sprout dynamics and suggest pulling activity. *Angiogenesis* **2020**, *23* (3), 315–324.
- (53) Wang, W. Y.; Jarman, E. H.; Lin, D.; Baker, B. M. Dynamic Endothelial Stalk Cell-Matrix Interactions Regulate Angiogenic Sprout Diameter. *Front. Bioeng. Biotechnol.* **2021**, *9*, 620128.
- (54) Pedersen, J. A.; Boschetti, F.; Swartz, M. A. Effects of extracellular fiber architecture on cell membrane shear stress in a 3D fibrous matrix. *J. Biomech.* **2007**, *40* (7), 1484–1492.
- (55) Zheng, Y.; Wang, S.; Xue, X.; Xu, A.; Liao, W.; Deng, A.; Dai, G.; Liu, A. P.; Fu, J. Notch signaling in regulating angiogenesis in a 3D biomimetic environment. *Lab Chip* **2017**, *17* (11), 1948–1959.

- (56) Shahhosseini, M.; Beshay, P. E.; Akbari, E.; Roki, N.; Lucas, C. R.; Avendano, A.; Song, J. W.; Castro, C. E. Multiplexed Detection of Molecular Interactions with DNA Origami Engineered Cells in 3D Collagen Matrices. ACS Appl. Mater. Interfaces 2022, 14 (50), 55307–55319.
- (57) Beshay, P. E.; Cortes-Medina, M. G.; Menyhert, M. M.; Song, J. W. The Biophysics of Cancer: Emerging Insights from Micro- and Nanoscale Tools. *Adv. NanoBiomed Res.* **2022**, *2* (1), 2100056.
- (58) Tien, J.; Ghani, U.; Dance, Y. W.; Seibel, A. J.; Karakan, M. C.; Ekinci, K. L.; Nelson, C. M. Matrix Pore Size Governs Escape of Human Breast Cancer Cells from a Microtumor to an Empty Cavity. *iScience* **2020**, 23 (11), 101673.
- (59) Liu, C.; Lewin Mejia, D.; Chiang, B.; Luker, K. E.; Luker, G. D. Hybrid collagen alginate hydrogel as a platform for 3D tumor spheroid invasion. *Acta Biomater.* **2018**, *75*, 213–225.
- (60) Jung, H. Hyaluronidase: An overview of its properties, applications, and side effects. *Arch Plast Surg* **2020**, *47* (4), 297–300.
- (61) Whatcott, C. J.; Han, H.; Posner, R. G.; Hostetter, G.; Von Hoff, D. D. Targeting the tumor microenvironment in cancer: Why hyaluronidase deserves a second look. *Cancer Discovery* **2011**, *1* (4), 291–296.
- (62) Rahbari, N. N.; Kedrin, D.; Incio, J.; Liu, H.; Ho, W. W.; Nia, H. T.; Edrich, C. M.; Jung, K.; Daubriac, J.; Chen, I.; Heishi, T.; Martin, J. D.; Huang, Y.; Maimon, N.; Reissfelder, C.; Weitz, J.; Boucher, Y.; Clark, J. W.; Grodzinsky, A. J.; Duda, D. G.; Jain, R. K.; Fukumura, D. Anti-VEGF therapy induces ECM remodeling and mechanical barriers to therapy in colorectal cancer liver metastases. Sci. Transl. Med. 2016, 8 (360), 360ra135.
- (63) Slevin, M.; Krupinski, J.; Gaffney, J.; Matou, S.; West, D.; Delisser, H.; Savani, R. C.; Kumar, S. Hyaluronan-mediated angiogenesis in vascular disease: Uncovering RHAMM and CD44 receptor signaling pathways. *Matrix Biol.* **2007**, *26* (1), 58–68.
- (64) Chen, C. G.; Iozzo, R. V. Angiostatic cues from the matrix: Endothelial cell autophagy meets hyaluronan biology. *J. Biol. Chem.* **2020**, 295 (49), 16797–16812.
- (65) Folkman, J. What is the evidence that tumors are angiogenesis dependent? J. Natl. Cancer Inst. 1990, 82 (1), 4–6.
- (66) Ellis, L. M.; Hicklin, D. J. VEGF-targeted therapy: Mechanisms of anti-tumour activity. *Nat. Rev. Cancer* **2008**, 8 (8), 579–591.
- (67) Sledge, G. W. Anti-vascular endothelial growth factor therapy in breast cancer: Game over? *J. Clin. Oncol.* **2015**, 33 (2), 133–135.
- (68) Jayson, G. C.; Kerbel, R.; Ellis, L. M.; Harris, A. L. Antiangiogenic therapy in oncology: Current status and future directions. *Lancet* **2016**, 388 (10043), 518–529.
- (69) Helm, C.-L. E.; Fleury, M. E.; Zisch, A. H.; Boschetti, F.; Swartz, M. A. Synergy between interstitial flow and VEGF directs capillary morphogenesis in vitro through a gradient amplification mechanism. *Proc. Natl. Acad. Sci. U. S. A.* **2005**, *102* (44), 15779–15784.
- (70) Antoine, E. E.; Vlachos, P. P.; Rylander, M. N. Tunable Collagen I Hydrogels for Engineered Physiological Tissue Micro-Environments. *PLoS One* **2015**, *10* (3), e0122500.